Journal of
Computational and Theoretical Nanoscience
Vol. 3, 1–10, 2006

Selectivity of the Chelator-Protein Interactions: A High Level Quantum Chemistry Study

Stepan G. Stepanian,[1] Bartosz Trzaskowski,[2] Pierre A. Deymier,[3] Roberto Guzman,[4] and Ludwik Adamowicz[5,*]

[1] *Institute for Low Temperature Physics and Engineering, National Academy of Sciences of Ukraine, 47, Lenin Avenue, 61103, Kharkov, Ukraine*
[2] *Faculty of Chemistry, Warsaw University, Pasteura 1, 02-093 Warsaw, Poland*
[3] *Department of Materials Science and Engineering, University of Arizona, Tucson, Arizona 85721, USA*
[4] *Department of Chemical and Environmental Engineering, University of Arizona, Tucson, Arizona 85721, USA*
[5] *Department of Chemistry, University of Arizona, Tucson, Arizona 85721, USA*

We have employed correlated *ab-initio* and density functional theory (DFT) calculations to elucidate the selectivity of the interactions between chelators, which include $-N-(CH_2-COO^-)_n$ fragments and which coordinate di- and trivalent transition metal atoms and amino acids, with electron donor residues (histidine, cystein, methionine). The aim of the study is to initiate compilation of a database for such interactions based on the results obtained from the calculations. We found that an optimal (reliable and yet not too computationally damaging) approach for obtaining accurate interaction energies between chelators and amino acid residues involves an equilibrium geometry calculation at the DFT/6-31G* (for C, N, O, S, H atoms)/VTZ (for metal atoms) level of theory followed by a MP2 energy calculation performed at the DFT equilibrium geometry with the aug-cc-pVDZ|VTZ basis set. The most accurate interaction energies were obtained when the water molecules belonging to the first coordination sphere were included in the calculations. Also, accounting for the zero-point vibrational energy correction and the basis set superposition energy correction aided the accuracy of the calculations. The interaction energy calculations performed for the chosen set of chelators, metal ions (Zn^{2+}, Co^{2+}, Fe^{2+}, Ni^{2+}, Cu^{2+}, Pd^{2+}, Cd^{2+}), and amino acid residues allowed us to elucidate the selectivity of the interactions.

Keywords: Chelator, Selectivity, Transition Metals, Hystidine, Cystein, Methionine, IDA, Quantum-Chemical Calculations.

RESEARCH ARTICLE

1. INTRODUCTION

The main target of this work is the interaction between metal-loaded chelators and amino-acids-carrying residues that are able to form strong bonds with *d* and/or *f* metal ions. There is growing interest in these systems due to their importance in numerous applications such as: protein immobilization and purification,[1–6] DNA immobilization,[7,8] and the development of nanoscale biosensors,[9–14] and electronic devices.[15,16] The basic idea of the applications is combining of unique physical and mechanical properties of the nanoscale materials with specificity and selectivity of the intermolecular interactions of biological molecules.

Although the number of possible combinations of various chelators, metal ions, and amino acids is large, the main attention in the present work is paid to two systems: IDA (iminodiacetic acid)-Cu(II), which has a high affinity to histidine[6,7,15,17–19] and NTA (nitrilotriacetate)-Ni(II), which is able to coordinate multihistidine tags.[1,5,10–15,20–22] Other less frequently used chelators and metal ions are ADA (*N*-(2-acetamide)-iminodiacetic acid),[23–25] DPA (di-(2-picolyl) amine),[26,27] TREN (tris(2-aminoethyl)-amine),[28–30] Zn(II),[7,27–31] Fe(II),[30] Co(II),[7,11,23,29–31] Pd(II),[29] Cd(II),[32] Mn(II),[30] Zr(IV),[33] Hf(IV),[33] as well as some lanthanides (Sm, Eu, Gd, Tb, Ho, Pr).[34,35] In spite of the numerous experimental studied of the metal loaded chelators the theoretical investigations of these systems are very limited. Taratiel et al.[36] applied multi-configurational perturbation theory (CASPT2) to study the ferromagnetic coupling in systems including transition metals and TREN. Also the electronic spectra of the ligated IDA-Cu complex were studied by means of the configuration interaction (CIS) method.[37] The lack

*Author to whom correspondence should be addressed.

1546-198X/2006/3/001/010 doi:10.1166/jctn.2006.006

of balance between the available extensive experimental studies and the limited theoretical studies may be due to several reasons which have hampered application of computational methods to study chelator systems. First, only high level quantum chemical methods accounting for electron correlation energy are adequate to describe the interactions in the transition metal containing chelating systems. Secondly, these systems are usually large and they take significant amounts of computer time to calculate. Thirdly, the influence of the solvent should be taken into account in the computational model in order to adequately describe these systems. As a result the detailed information about selectivity of the interactions between chelators and ligands (amino acid residues are among the most frequent ligands) has not been obtained using the computational methods at adequate levels of theory.

Recently we presented an *ab-initio* computational approach directed towards building a data base of immobilized ligands targeting proteins.[38] The interaction between histidine and IDA chelator attached to the gold surface and loaded with different divalent metal ions was studied using the Density Functional Theory (DFT) method. We found that the strength of the interaction is neither very sensitive to removing the gold surface from the calculated model nor to removing the alkyl chain connecting the chelator to the surface.

The main goal of the present work has been to determine the selectivity of intermolecular interactions in the chelator-metal-amino acid complexes for the most common chelators and the commonly used transition metals. To achieve this goal we first determined which quantum chemistry methods are capable of correctly predicting the selectivity of the interactions between chelators containing transition metals and the amino acids residues. To accomplish that we performed a series of test calculations of the interaction energies for some chelators, metal atoms (Zn^{2+}, Cd^{2+}, Fe^{2+}, Ni^{2+}, Cu^{2+}, Pd^{2+}, Cd^{2+}), and amino acids (histidine, cysteine, methionine which are modeled by imidazole, CH_2CH_2SH and $CH_2CH_2SCH_3$, respectively). Next, based on the results of the calculations, we determined the optimal level of theory which is the least computationally expensive yet able to correctly predict the interaction energies. In this analysis we performed calculations using various methods (DFT, MP2, MP4), as well as basis sets (Ahlrichs' VTZ, Stuttgart RSC 1997 ECP) for metal atoms and the 6-31G*, aug-cc-pVDZ, aug-cc-pVTZ basis sets for C, N, O, S, H. Another issue in the analysis was to select a realistic molecular model for the studied systems to be used in the calculations. In the process of identifying such a model calculations were performed for simple chelator-metal-amino-acid systems, as well as for systems including up to 34 water molecules solvating the complex. Additional calculations have also been performed for solvated chelator systems using the Polarizable Continuum Model (PCM) representing the aqueous environment.

Table I. Basis sets used in calculations.

Basis set abbreviation	Atoms: C N O S H	Atoms: Fe, Ni, Co, Cu, Zn	Atoms: Cu, Zn, Pd, Cd
BS1	6-31G* Refs. [42]–[44]	Ahrlich's VTZ Ref. [48]	—
BS2	aug-cc-pVDZ Refs. [45]–[47]	Ahrlich's VTZ	—
BS3	aug-cc-pVTZ Refs. [45]–[47]	Ahrlich's VTZ	—
BS4	6-31G*	—	Sttutgartt RSC 1997 ECP Refs. [49, 50]

2. COMPUTATIONAL DETAILS

The geometries of the studied systems were first fully optimized at the DFT level of theory. The DFT calculations were carried out with the three-parameter density functional, usually abbreviated as B3LYP, which includes Becke's gradient exchange correction,[39] the Lee, Yang, Parr correlation functional[40] and the Vosko, Wilk, and Nusair correlation functional.[41] The geometries of several selected systems were also optimized at the MP2 level. Next, harmonic frequency calculations were performed for the equilibrium DFT geometries and the frequency results were used to account for the zero-point vibrational energy (ZPVE) correction. Additionally, single point energy calculations were performed at the MP2 and MP4 levels of theory for the DFT geometries and at the MP4 level for the MP2-optimized geometries. In the calculations we used four basis sets denoted as BS1, BS2, BS3, and BS4, respectively. They are described in Table I. We used the Ahlrichs' VTZ and the Stuttgart RSC ECP 1997 basis sets since they are available for most of the transition metal atoms. Calculations were also performed for the complexes with addition of one to seven water molecules. To more accurately account for the solvation effects we also employed the PCM method.[51–54] All interaction-energy calculations were performed with accounting for the BSSE correction using the standard counterpoise correction method.[55] All calculations were performed using the Gaussian 03 quantum chemistry package.[56]

3. RESULTS AND DISCUSSION

3.1. Lowest Energy Electronic States

The common problem in a computational study of transition-metal-containing compounds is finding their lowest-energy electronic states. In the present calculations we first needed to determine the lowest-energy electronic state of the metal ion chelated in a particular moiety. This determination involved comparing the energies of the simple neutral IDA-Me(II) systems (Fig. 1) containing different metals. Thus, for each metal complex we performed calculations for three electronic states: singlet, triplet, and pentuplet for systems with even number of electrons

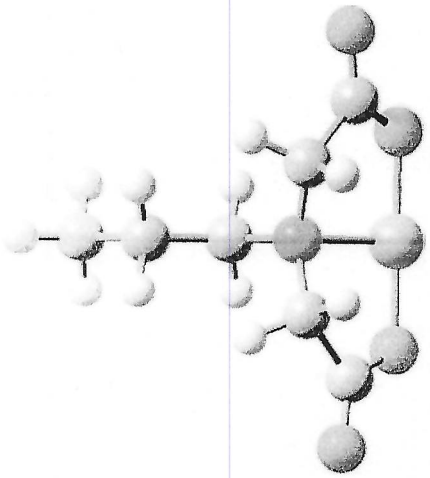

Fig. 1. Structure of the metal-containing chelator iminodiacetic acid (N—blue, O—red, C—grey, H—white).

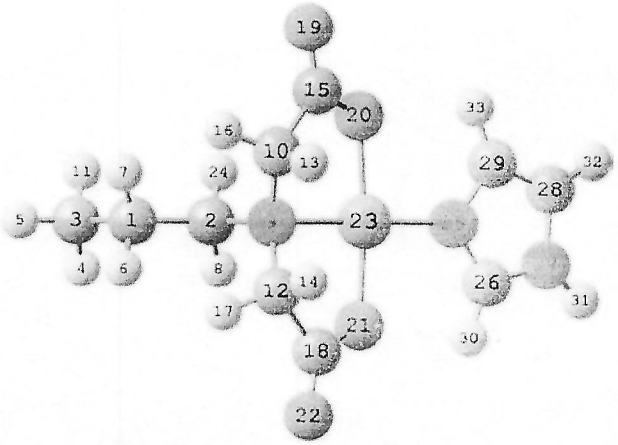

Fig. 2. Structure of the IDA-Cu-IM complex.

(Me = Fe(II), Ni(II), Zn(II), Pd(II), Cd(II)), and doublet, quadruplet, and sextuplet for systems with odd numbers of electrons (Me = Co(II) and Cu(II)). The energies were calculated for geometries fully optimized at the B3LYP/B1 (Me = Fe, Co, Ni, Cu) and B3LYP/B4 (Me = Cd, Pd) levels of theory. The resulting energies are collected in Table II. We found that the electronic states with the lowest energies are all singlets for the Zn, Pd, and Cd complexes; all doublets for Cu complexes; all triplets for Ni complexes, all quadruplets for Co complexes, and all pentuplets for Fe complexes. We were not able to determine the energies for the sextuplet states of the IDA-Co and IDA-Cu complexes since these systems are not stable. Next we verified the results by performing additional calculations for each system using the CIS/BS1 method. The obtained multiplicities were used in further calculations for all metals except Fe. For Fe we found that addition to the IDA-Fe(II) system of a ligand may change its lowest-energy electronic state to a triplet.

3.2. Level of Theory and Basis Set Variations

As we stated above, our aim in this work is to develop a database for the chelator-metal-protein interactions. Accomplishing this task requires performing numerous calculations. Thus in the first step of the study we focused on determining an optimal strategy for such calculations. By 'optimal' we mean as accurate as possible yet not too computationally expensive. More specifically we needed to chose an approach including a quantum chemical method and a basis set which are capable of providing accurate structures and harmonic frequencies (which are necessary for accounting for ZPVE correction) of the studied complexes, as well a method/basis set combination which is capable of predicting accurate interaction energies calculated for the geometries obtained in the first step. In the analysis we compared the accuracy of the B3LYP/BS1 and MP2/BS1 methods for geometry optimization, and the accuracy of the B3LYP, MP2, and MP4(SDQ) methods with different basis sets listed in Table I in the interaction energy calculations. The calculations were performed for the IDA-Cu-IM complex (Fig. 2). Imidazole (IM) in this complex models the histidine side chain.[38] The interaction energies were calculated for the following process: IDA-Cu + IM → IDA-Cu-IM. The interaction energies (BSSE and ZPVE corrected) obtained in the calculations are collected in Table III.

As seen from Table III, the interaction energies calculated for the B3LYP/BS1 and MP2/BS1 geometries are

Table II. Energies (a.u.) of different electronic states at fully optimized structures of the IDA-Me(II) complex calculated at the B3LYP level of theory. The 6-31G* basis set was used for C, N, O, and H atoms. Ahlrich's VTZ basis was used for Fe, Co, Ni, Cu, and Zn atoms. The Stuttgart RSC 1997 ECP basis set was used for Pd and Cd atoms.

	Multiplicity					
Metal	1	2	3	4	5	6
Fe	−1892.7343378	—	−1892.7705146	—	*−1892.7964271*	—
Co	—	−2011.8371255	—	*−2011.8414357*	-	N/A[a]
Ni	−2137.3795124	—	*−2137.3875483*	—	−2137.2382451	—
Cu	—	*−2269.5490731*	—	−2269.3866848	—	N/A[a]
Zn	*−2408.4217231*	—	−2408.3246363	—	−2408.1712338	—
Pd	*−756.9491239*	—	−756.9249084	—	−756.7733393	—
Cd	*−796.8170353*	—	−796.7765345	—	−796.6356741	—

[a]System is not stable. Energies calculated for IDA-Co and IDA-Cu sextuplet states using quadruplet (IDA-Co) and doublet (IDA-Cu) geometries are −2011.6702938 and −2269.1587814 a.u., respectively.

Table III. Interaction energies (kJ/mol, ZPVE, and BSSE corrected) obtained for the IDA-Cu(II)-Im complex at different levels of theory using different basis sets.

	Geometry	
Method	B3LYP/BS1	MP2/BS1
B3LYP/BS1	−121.72	−123.43
B3LYP/BS2	−128.27	−129.25
B3LYP/BS3	−128.43	−129.58
MP2/BS1	−147.75	−145.34
MP2/BS2	−158.06	−154.49
MP4/BS1	−145.67	−143.65

similar and the results do not depend much on the method and on the basis set used in the calculations; the difference is only about 1–3 kJ/mol. This value is within the standard error of the B3LYP method. This indicates that the B3LYP method is able to predict structures with similar accuracy as the MP2 method which is much more computationally expensive than B3LYP. Thus we concluded that the MP2 optimization can be avoided and replaced by the B3LYP optimization. In Table IV we compare selected structural parameters of the IDA-Cu-IM complex obtained at the B3LYP/BS1 and MP2/BS1 levels of theory. It can be seen that the geometries predicted by both methods are very similar. The differences are within 0.02 Å for the bond lengths, 0.5 degrees for the bond angles and 3 degrees for the dihedral angles. This confirms the ability of the B3LYP method to accurately predict the geometries of chelator-transition metal complexes.

Unfortunately the lack of experimental data on the IDA-Cu-IM structures precludes direct comparison between the

Table IV. Selected structural parameters (angstrom and degrees) of the IDA-Cu-Im complex fully optimized at the B3LYP/BS1 and MP2/BS1 levels of theory. Atom numbering is shown in Figure 2.

	Method	
Parameter	B3LYP/BS1	MP2/BS1
Bond lengths		
$Cu\text{-}N_9$	2.025	2.000
$Cu\text{-}O_{20}$	1.907	1.894
$Cu\text{-}O_{21}$	1.914	1.899
$Cu\text{-}N_{25}$	1.975	1.963
$C_{15}\text{-}O_{20}$	1.307	1.313
$C_{18}\text{-}O_{21}$	1.307	1.314
Angles		
$N_9\text{-}Cu\text{-}O_{20}$	85.89	86.10
$N_9\text{-}Cu\text{-}O_{21}$	85.70	85.91
$N_{25}\text{-}Cu\text{-}O_{20}$	95.13	94.82
$N_{25}\text{-}Cu\text{-}O_{21}$	93.31	93.22
$C_{15}\text{-}O_{20}\text{-}Cu$	114.95	114.84
$C_{18}\text{-}O_{21}\text{-}Cu$	114.96	114.93
Dihedrals		
$N_9\text{-}Cu\text{-}O_{20}\text{-}C_{15}$	17.61	15.69
$N_9\text{-}Cu\text{-}O_{21}\text{-}C_{18}$	−17.86	−15.70
$N_{25}\text{-}Cu\text{-}O_{20}\text{-}C_{15}$	−163.94	−167.09
$N_{25}\text{-}Cu\text{-}O_{21}\text{-}C_{18}$	163.73	167.09
$O_{19}\text{-}C_{15}\text{-}O_{20}\text{-}Cu$	175.82	178.49
$O_{22}\text{-}C_{18}\text{-}O_{21}\text{-}Cu$	−175.31	−178.19

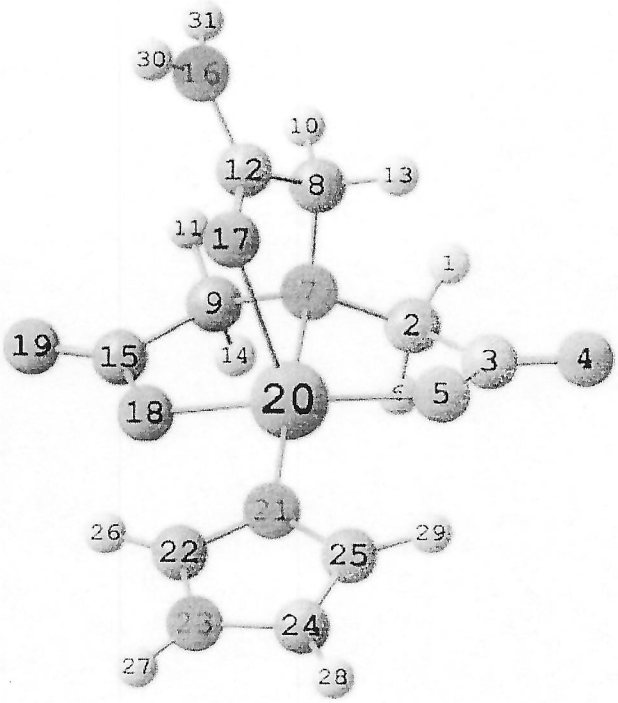

Fig. 3. Structure of the ADA-Cu-IM complex.

observed and the predicted structures. However we can use the available results of the X-ray diffraction study of the ADA-Cu-IM complex (ADA = *N*-carbamoylmethyl-iminodiacetic acid)[25] which is similar to the IDA-Cu-IM complex (Fig. 3) to make a comparison. In the comparison, the geometry of the ADA-Cu-IM complex was fully optimized at the B3LYP/BS1 level of theory and the calculated structure, as well as the experimental data are presented in Table V (only for the Cu environment). As it is seen, both sets of parameters are in good agreement. It should be remembered that the observed structure is disturbed by strong intermolecular interactions in the solid ADA-Cu-IM. The mean differences for the bond lengths and for the

Table V. Selected structural parameters (angstrom and degrees) of the ADA-Cu-Im complex calculated at the B3LYP/BS1 level of theory. Atom numbering is shown in Figure 3.

Parameter	Observed[25]	Calculated
Bond lengths		
$Cu\text{-}O_5$	1.943	1.926
$Cu\text{-}N_{21}$	1.960	1.976
$Cu\text{-}O_{18}$	1.964	1.926
$Cu\text{-}N_7$	2.040	2.058
$Cu\text{-}O_{17}$	2.322	2.407
Angles		
$O_5\text{-}Cu\text{-}N_{21}$	98.03	95.33
$O_5\text{-}Cu\text{-}O_{18}$	162.45	164.83
$O_{18}\text{-}Cu\text{-}N_{21}$	94.55	93.03
$O_5\text{-}Cu\text{-}N_7$	83.80	84.27
$O_5\text{-}Cu\text{-}O_{17}$	103.25	103.68
$N_{21}\text{-}Cu\text{-}O_{17}$	93.25	92.74
$O_{17}\text{-}Cu\text{-}O_{18}$	88.12	86.49
$N_7\text{-}Cu\text{-}O_{17}$	82.56	79.45

RESEARCH ARTICLE

bond angles calculated for the whole set of the structural parameters are 0.02 Å and 1.4°, respectively. The comparison demonstrates that the B3LYP/BS1 method is capable of accurately predicting the geometries of chelated transition metal systems.

On other hand the data presented in Table III demonstrate that the interaction energy significantly depends on the method and the basis set used in the calculations. Increasing the basis set size from BS1 to BS2 gives a lowering of the energy by 6.55 kJ/mol at the B3LYP level and by 10.31 kJ/mol at the MP2 level. However further increasing of the basis set to BS3 leads only to a small energy change. The difference between the interaction energies calculated at the B3LYP/BS2 and B3LYP/BS3 levels of theory is only 0.16 kJ/mol. This demonstrates that the BS2 basis set (aug-cc-pVDZ for hydrogens and second row atoms; Ahlrich's VTZ for metal atoms) is adequate for the calculations performed in this work.

The comparison of the interaction energies (Table III) obtained at the different levels of theory (B3LYP, MP2, MP4(SDQ)) demonstrates an important difference between the B3LYP and MP2 calculations. MP2/BS1 and MP2/BS2 interaction energies are lower than the corresponding B3LYP energies by 26.03 and 29.79 kJ/mol, respectively (for the B3LYP/BS1 geometry). On the other hand the same difference between MP2/BS1 and MP4(SDQ)/BS1 interaction energies is only 2.08 kJ/mol. It means that the accuracy of the MP2 method is probably sufficient to predict correct interaction energies in the chelator-metal-amino acid complexes.

In conclusion, we can say that the optimum approach to study the energy selectivity of the interactions between transition-metal-containing chelators and amino acids needs to include: (a) a geometry optimization performed at the B3LYP/BS1 level of theory, (b) a single-point energy calculation at the B3LYP BS1 geometry performed at the MP2/BS2 level of theory. Further increasing of the basis set size or utilization of a more precise computational method is likely to lead to an insignificant increase of the accuracy of the calculated energies at the expense of a considerably larger use of computer resources.

3.3. Models

Next issue which needed to be addressed in the study was choosing an appropriate molecular model to realistically describe the chelating process. The main problem here was accounting for the influence of the solvent (water) on the interaction energy between the chelator and the amino acid residue. To solve this problem we tested several models. We started from the simplest one which corresponded to the gas phase interaction. Next we gradually increased the level of complexity of the model by: (i) explicitly adding water molecules and increasing their number, (ii) accounting for the presence of the solvent using the continuum-model calculations, (iii) combining the approaches (i) and (ii).

Table VI. Interaction energies (kJ/mol) calculated at the B3LYP/BS1 level of theory for the IDA-Cu-IM complex using Models 1–5.

	IDA-Cu-IM (Models 1–3) or IDA-Cu-IM-6W (Models 4–5)	IDA-Cu-W (Models 1–3) or IDA-Cu-W-6W (Models 4–5)	ΔE_{IM-W}
Model 1	−121.72		
Model 2	−121.72	−69.29	−52.43
Model 3	−90.59	−57.37	−33.25
Model 4	−130.89	−73.17	−57.72
Model 5	−95.04	−59.06	−35.98

We tested the reliability of the models using the same complex as in the previous section, namely IDA-Cu-IM (Fig. 2). The geometry of the complex for each model was first fully optimized at the B3LYP/BS1 level of theory and the interaction energies were calculated with the BSSE and ZPVE corrections. All calculated interaction energies are presented in Table VI.

In Model 1 the interaction energy was calculated as a difference between the energy of the Chelator-Metal-Amino Acid (AA) complex and the sum of the energies of the Chelator-Metal and amino-acid subsystems. This interaction energy is equivalent to the following dissociation process:

$$\text{IDA-Cu} + \text{IM} \rightarrow \text{IDA-Cu-IM}$$

Since the model was discussed in details above we just mention that the interaction energy is −121.72 kJ/mol, and this value will be used as the reference point for the rest of the models.

In Model 2 the interaction energy was calculated as the difference between the interaction energies obtained for the Chelator-Metal-AA and Chelator-Metal-Water (W) complexes. More precisely the interaction energy was calculated as the energy change due to the replacement of the water molecule by the amino acid residue. The process may be represented by the following reaction:

$$\text{IDA-Cu-W} + \text{IM} \rightarrow \text{IDA-Cu-IM} + \text{W}$$

or in the form of two reactions as:

$$\text{IDA-Cu-W} \rightarrow \text{IDA-Cu} + \text{W}$$

$$\text{IDA-Cu} + \text{IM} \rightarrow \text{IDA-Cu-IM}$$

The calculated structure of the IDA-Cu-W complex is shown in Figure 4. In Model 2 the interaction energy is always lower than in Model 1 by the interaction energy between the chelator and one water molecule. Model 2 allows us to determine if the complex formation is possible. It depends on the relative values of the interaction energies calculated for the first and the second reaction mentioned above. In the case of the IDA-Cu-IM complex the interaction between IDA-Cu and IM (−121.72 kJ/mol) is stronger than the interaction between IDA-Cu and W (−69.29 kJ/mol) by −52.43 kJ/mol. Such an approach to predicting the relative stability of IDA-Cu-IM with respect

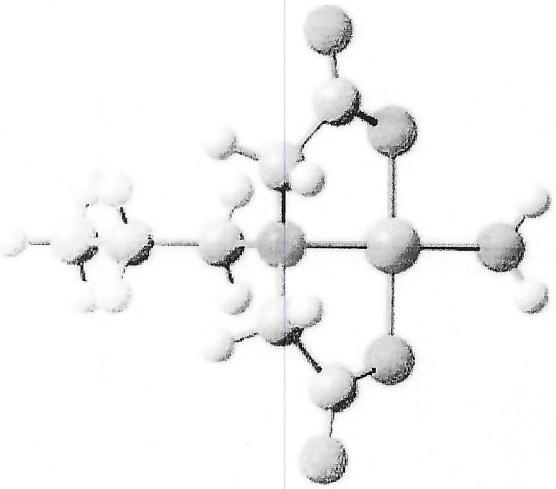

Fig. 4. Structure of the IDA-Cu-W complex.

to IDA-Cu-W is likely to be more precise than calculating the interaction energies directly due to the expected cancellation of possible inaccuracies of the methods and the models used in the calculations. Those methods and models were similar for both complexes.

Model 3 is similar to Model 2, but, instead of including a single water molecule to represent the salvation, the PCM method is used. In this model we use the same geometries of the complexes as in Model 2. Accounting for the influence of the solvent reduces the interaction energies between the chelator (IDA-Cu) and the ligands (IM, W) as compared with Model 2 by 31.13 and 11.82 kJ/mol, respectively. The resulting relative stability of IDA-Cu-IM with respect to IDA-Cu-W is also lower than for Model 2 and corresponding relative energy is −33.25 kJ/mol.

In Model 4 the first complete coordination sphere of the solvent surrounding the interaction site is explicitly added. For the IDA-Cu chelator it includes seven water molecules. In this model, the energy change is calculated for the following displacement reaction:

$$\text{IDA-Cu-7W} + \text{IM} \rightarrow \text{IDA-Cu-IM-6W} + \text{W}$$

or more precisely for the following two reactions:

$$\text{IDA-Cu-7W} \rightarrow \text{IDA-Cu-6W} + \text{W}$$

$$\text{IDA-Cu-6W} + \text{IM} \rightarrow \text{IDA-Cu-IM-6W}$$

The calculated structures of IDA-Cu-7W and IDA-Cu-IM-6W are shown in Figure 5. Each COO^- group of IDA coordinates 2 water molecules forming two strong hydrogen bonds between IDA oxygen atoms and the water hydrogens, as well as one hydrogen bond between the two water molecules. The COO^-–$(H_2O)_2$ fragments are very stable and remain unchanged in the IDA-Cu-IM-6W complex after the replacement reaction. To determine the influence of the solvation more precisely we performed an additional calculation of the IDA-Cu-IM-6W complex augmented with the second solvation sphere which consists

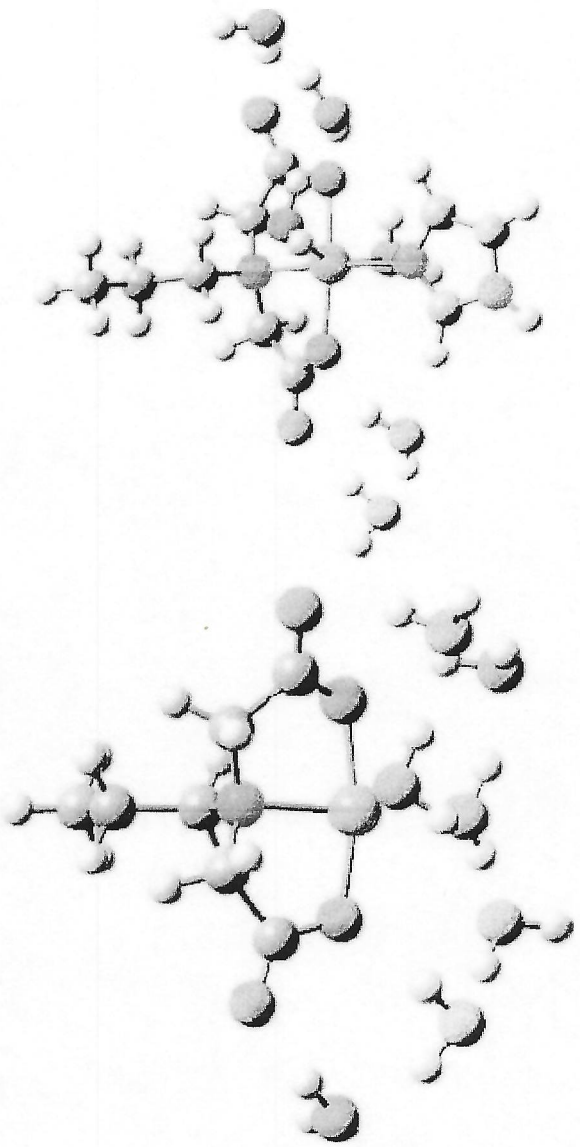

Fig. 5. Structure of the IDA-Cu-7W (top) and IDA-Cu-IM-6W (bottom) complexes.

of as many as 28 water molecules. Its structure is shown in Figure 6. As seen, the COO^-–$(H_2O)_2$ fragments (water molecules are marked with red arrows in Fig. 6) also remain in the IDA-Cu- IM-34W complex after the replacement reaction. In the IDA-Cu-IM-6W complex there are two water molecules strongly bonded to the central copper atom. These two water molecules are also present in the IDA-Cu-IM-34W complex. They are marked with green arrows in Figure 6. It means that inclusion of additional water molecules does not significantly change the structure of the first coordination sphere.

However, addition of water molecules increases the interaction energies between the IDA-Cu-6W complex and imidazole or water as compared to Model 2. The interaction energies are −130.89 and −73.17 kJ/mol, respectively, and the relative energy is −57.72 kJ/mol—much higher than that of Model 2 by 5.29 kJ/mol.

RESEARCH ARTICLE

Fig. 6. Structure of the IDA-Cu-IM-34W complex. Arrows indicate water molecules included in Models 4 and 5. See explanation in text.

Model 5 is a combination of Models 3 and 4. In this model the first coordination sphere is included (Model 3) and the PCM method is used for representing the second and the higher solvation spheres (Model 4). The effect of the solvent on the interaction energies between the chelator (IDA-Cu-6W) and the ligands (IM and W) obtained in Model 5 is very close as that obtained in Model 3. Including the continuum solvation model in the calculation leads to decreasing interaction energies for IM and W by 35.85 and 14.11 kJ/mol, respectively. The corresponding energy decrease for Model 3 was 31.13 and 11.82 kJ/mol, respectively. The resulting relative energy of IDA-Cu-IM-6W with respect to IDA-Cu-7W is −35.98 kJ/mol and the difference between Models 3 and 5 is only 2.73 kJ/mol. It demonstrates that, although the addition of water molecules improves the accuracy of the calculated interaction energies between the chelator (IDA-Cu-6W) and the ligands (IM and W), the resulting relative energy does not change significantly.

3.4. Selectivity of the Interactions

The next step in the study was the investigation of the selectivity of the interactions between IDA-Me(II) chelators and several amino acids. The aim was to determine the combinations of metal ions and amino acid residues which have the relative stabilities significantly different from other complexes or which may be formed when the formation of complexes of the same metal ion with other amino acid residues or the same residue but with other metal ions is not energetically possible.

In the calculations the amino acids have been modeled by simpler compounds similar to the corresponding amino acid residues: hystidine by imidazole, cystein by CH_3CH_2SH, and methionine by $CH_3CH_2SCH_3$. The selectivity was studied for a set of transition metal ions: Cu^{2+}, Ni^{2+}, Co^{2+}, Zn^{2+}, Fe^{2+}, Pd^{2+}, Cd^{2+} that are usually used in chelators. Using the models described in the previous section we calculated the interaction energies for the transition metals and the amino-acid residues using the B3LYP method in the geometry optimization and the zero-point vibrational energy calculations and using the MP2 method in the single point energy calculations. In these calculations we used two basis sets-BS1 for Cu, Ni, Co, Zn, Fe, and BS4 for Pd, Cd and also for Cu, Zn. The basis sets are described in Table I. As it is seen, the only difference between the basis sets is related to the metal atoms. The all-electron Ahlrich's VTZ basis was used in the BS1 basis for the metal atoms, whereas in the BS4 basis we used the Stuttgart RSC ECP 1997 basis set with the effective core potentials for the internal electrons. In the following subsections we present the results obtained for the IDA-Me(II)-IM, IDA-Me(II)-CYS (CYS-cystein residue), IDA-Me(II)-MET (MET-methionine residue) systems.

3.4.1. *IDA-Me(II)-IM*

The structures of the complexes predicted for all considered metal atoms are similar. In Figure 1 we present the structure of IDA-Cu-IM as an example. The calculated interaction energies are collected in Table VII. These data demonstrate that imidazole has a high affinity towards the IDA ligand. For all complexes, the interaction energies with imidazole are much higher than with water and they depend very little on the metal used in the chelator. The relative stability ($\Delta E_{IM\text{-}W}$) calculated at the MP2 level of theory is the lowest for the IDA-Zn-IM complex (−50.25 kJ/mol). The relative energies calculated for Cu, Ni, Co, Fe, and Cd are close (within −55 to −65 kJ/mol). For the IDA-Pd-IM complex the calculations predict the highest relative energy of almost −90 kJ/mol. Although

Table VII. Interaction energies (kJ/mol) of the IDA-Me(II)-IM complexes calculated at the B3LYP and MP2 levels with the BS1 and BS4 basis sets for the geometries fully optimized at the B3LYP/BS1 and BS4 level of theory.

	IDA-Me-IM		IDA-Me-W		$\Delta E_{IM\text{-}W}$	
Metal	MP2	DFT	MP2	DFT	MP2	DFT
BS1						
Cu	−147.75	−121.72	−87.85	−69.29	−59.90	−52.43
Ni	−132.03	−107.16	−77.72	−62.49	−54.31	−34.67
Co	−128.38	−108.63	−71.00	−57.06	−57.38	−51.57
Zn	−113.79	−100.04	−63.54	−56.66	−50.25	−43.38
Fe	−178.33	−190.80	−113.21	−116.99	−65.12	−73.01
BS4						
Cu	−147.10	−126.41	−84.54	−72.00	−62.56	−56.41
Pd	−187.90	−176.07	−98.05	−95.13	−89.85	−80.94
Cd	−119.48	−108.59	−60.38	−56.17	−59.10	−52.42
Zn	−118.82	−114.48	−61.32	−62.15	−57.50	−52.33

RESEARCH ARTICLE

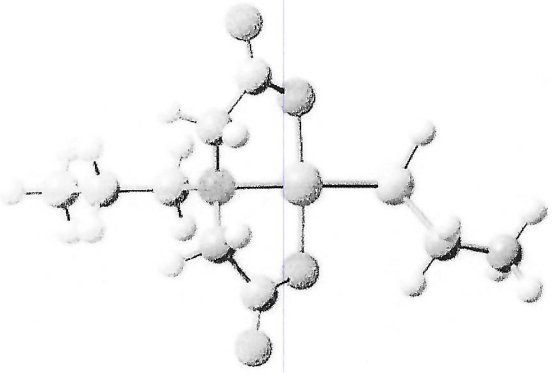

Fig. 7. Structure of the IDA-Cu-CYS complex.

the relative stabilities calculated for the set on transition metals are different they all are high enough to conclude that the histidine side chain is able to effectively interact with the IDA chelator independently of the metal atom ligated by the chelator.

3.4.2. IDA-Me(II)-CYS and IDA-Me(II)-MET

The predicted structures of the IDA-Cu-CYS and IDA-Cu-MET complexes are presented in Figures 7 and 8, respectively. The structures of the complexes containing other metals are similar. The interaction energies obtained for these complexes are presented in Tables VIII and IX IDA-Me(II)-CYS and IDA-Me(II)-MET, respectively. They are different from the ones obtained for the imidazole (hystidine) complexes. First of all we should note that both interaction energies (E_{CYS}, E_{MET}) and the relative stabilities ($\Delta E_{CYS\text{-}W}$ $\Delta E_{MET\text{-}W}$) are significantly lower in absolute values than the respective results for the imidazole complexes. Moreover, as seen from Tables VIII and IX, in several cases the interaction energies predicted for IDA-Me(II)-CYS and IDA-Me(II)-MET are higher than the ones predicted for IDA-Me(II)-W. It means that in these cases the formation of complexes may not be possible. We also can conclude that cystein residue chain demonstrates preferable addition to Pd and that cystein and methionine side chain to Pd and Fe. The corresponding interaction energy

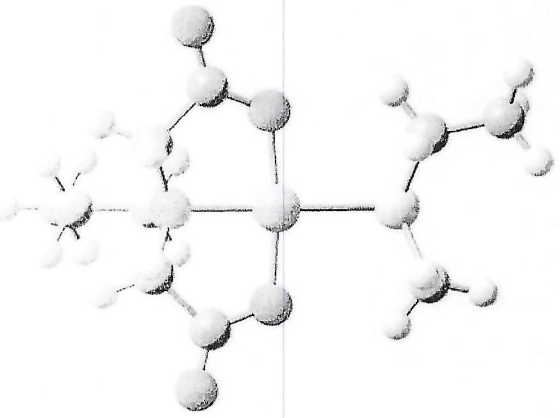

Fig. 8. Structure of the IDA-Cu-MET complex.

Table VIII. Interaction energies (kJ/mol) of the IDA-Me(II)-CYS complexes calculated at the B3LYP and MP2 levels with the BS4 basis set for geometries, fully optimized at the B3LYP/BS4 level of theory.

	IDA-Me-CYS		IDA-Me-W		$\Delta E_{CYS\text{-}W}$	
Metal	MP2	DFT	MP2	DFT	MP2	DFT
Cu	−79.09	−71.84	84.54	−72.00	+5.45	+0.16
Pd	−135.78	−130.70	−98.05	−95.13	−37.73	−35.57
Cd	−61.99	−59.94	−60.38	−56.17	−1.61	−3.73
Zn	−65.79	−62.42	−61.32	−62.15	−4.47	−0.27
Fe	−111.84	−92.72	−116.05	−89.04	+4.21	−8.68
Ni	−68.95	−64.20	−76.48	−70.15	+7.53	+5.95
Co	−75.40	−70.22	−78.88	−71.79	+3.48	+1.57

in this case is much higher than those predicted for the other metal atoms.

The calculated interaction energies between the IDA-Me(II) chelators and four different ligands (imidazole, CH_2CH_2SH, $CH_2CH_2SCH_3$, and water) demonstrate that imidazole has the strongest affinity to all chelators. The interaction energies calculated for the IDA-Me(II)-IM complexes are within −100 to −200 kJ/mol and are much higher than ones calculated for the other ligands. This effect can be explained by the presence of two additional C–H···O contacts in the IDA-Me(II)-IM complexes (see Fig. 2) with H···O distances in the range of 2.4–2.5 Å. Although the C–H···O interactions are usually weaker than the conventional N–H···O and O–H···O hydrogen bonds, in the complexes studied they are enhanced due to high negative charges on the O atoms: the Mulliken atomic charges calculated at the B3LYP/BS1 level of theory for the O atoms involved in the interaction in the IDA-Cu-IM complex are −0.65 a.u.

The same reasoning (additional intermolecular contacts) may explain why interaction energies in the IDA-Me(II)-MET complexes are always higher than in the IDA-Me(II)-CYS complexes. As seen in Figures 7 and 8, there is an additional C–H···O contact in IDA-Me(II)-MET as compared to IDA-Me(II)-CYS. It results in higher interaction energies predicted for IDA-Me(II)-MET by 10–15 kJ/mol (Tables VIII and IX).

The analysis of the calculated interaction energies and the Me(II)-X bonds lengths (Table X), where Me(II) is

Table IX. Interaction energies (kJ/mol) of the IDA-Me(II)-MET complexes calculated at the B3LYP and MP2 levels with the BS4 basis set for geometries fully optimized at the B3LYP/BS4 level of theory.[a]

	IDA-Me-MET		$\Delta E_{MET\text{-}W}$	
Metal	MP2	DFT	MP2	DFT
Cu	−93.98	−83.47	−9.44	−11.47
Pd	−155.31	−146.00	−57.26	−50.87
Cd	−76.27	−72.69	−15.89	−16.52
Zn	−81.83	−76.48	−20.51	−14.33
Fe	−129.32	−105.96	−13.27	−16.92
Ni	−82.95	−74.33	−6.47	−4.18
Co	−89.74	−82.12	−10.86	−10.33

[a]Interaction energies for the IDA-Me-W complexes are presented in Table VIII.

Table X. Interaction energies (IE, kJ/mol) and distances between the metal atom and the ligand (R_{Mc-X}, Å. X = N for imidazole, S for cystein and methionine, O for water).

	IDA-Me(II)-IM[a]		IDA-Me(II)-W[a]		IDA-Me(II)-CYS[b]		IDA-Me(II)-MET[b]	
Metal	IE	R_{Mc-N}	IE	R_{Mc-O}	IE	R_{Mc-S}	IE	R_{Mc-S}
Fe	−178.33	1.961	−113.21	1.967	−97.52	2.335	−109.45	2.328
Cu	−147.75	1.975	−87.85	2.025	−79.09	2.392	−93.98	2.378
Ni	−132.03	2.008	−77.72	2.059	−76.57	2.432	−82.95	2.426
Co	−128.38	2.057	−71.00	2.098	−75.40	2.431	−89.74	2.422
Zn	−113.79	2.091	−63.54	2.100	−65.79	2.446	−81.83	2.438

[a]Calculated at the MP2/BS1 level of theory. [b]Calculated at the MP2/BS4 level of theory.

the third row transition metal (Fe, Cu, Ni, Co, Zn) and X is the ligand atom forming the bond with the metal ion (N, O, S), demonstrates that correlation exists between these parameters. The shorter bond length corresponds to higher interaction energy. Thus the highest interaction energies and the shortest bond lengths are predicted for the IDA-Fe(II)-Ligand complexes while the IDA-Zn(II)-Ligand complexes has the lowest interaction energies and the longest bond lengths.

4. CONCLUSIONS

In this work we employed correlated high-level quantum-chemical calculations to study the selectivity of the interactions between transition metal containing chelators and amino acids. We tested the accuracy of various methods in predicting structures and interaction energies of such systems and we found that these properties may be efficiently calculated using a two-step approach: the first step involves the geometry optimization at the DFT/B3LYP level of theory with the 6-31G* basis set for non-transition metal atoms and the Ahlrichs' VTZ or the Stuttgart RSC ECP 1997 basis sets for the transition metal atoms; and the second step involves single point energy calculations performed for the DFT/B3LYP geometries at the MP2 level of theory with the Ahlrichs' VTZ or the Stuttgart RSC ECP 1997 basis set for the transition metal atoms and the aug-cc-pVDZ basis set for the non-transition metal atoms. We also tested the reliability of various models for accounting for the water environment in the calculations of the chelating systems. We found that using the PCM method and explicit addition of water molecules to the systems improves the accuracy of the calculated interaction energies. We noted that the interaction energy difference between the system where we explicitly included the first water coordination sphere (Model 5) and the system with only one added water molecule (Model 3) is not significant. This difference is within only 5% as calculated for the IDA-Cu-IM complex.

The calculations of the interaction energies performed for the IDA chelator and a set of transition metals (Cu, Ni, Co, Zn, Fe, Cd, Pd) and a set of amino acid residues (Histidine, Cystein, Methionine) demonstrated that the histidine side chain (imidazole) can efficiently connect to IDA with all the transition metals studied, although the resulting energies vary from −50 to −90 kJ/mol. We also noticed that cystein and methionine show clear preference to interact with the IDA-Pd complex.

Acknowledgment: We acknowledge financial support from NSF/NIRT Grant 0303863.

References

1. R. Janknecht, G. de Martynoff, J. Lou, R. A. Hipskind, A. Nordheim, and H. G. Stunnenberg, *Proc. Natl. Acad. Sci. USA* 88, 8972 (**1991**).
2. S. F. J. Le Grice and F. Gruninger-Leitch, *Eur. J. Biochem.* 187, 307 (**1990**).
3. V. M. Keivens, Ill, J. E. Hale, K. K. Nakamura, R. A. Jue, S. Cheng, E. D. Melcher, B. Drake, and M. C. Smith, *Biophys. J.* 64 (**1993**).
4. K. M. Ueda, P. W. Gout, and L. Morganti, *J. Chromatography A* 988, 1 (**2003**).
5. S. A. Lauer and J. P. Nolan, *Cytometry* 48, 136 (**2002**).
6. H. Chaouk and M. T. W. Hearn, *J. Biochem. Biophys. Methods* 39, 161 (**1999**).
7. J. C. Murphy, D. L. Jewell, K. I. White, G. E. Fox, and R. C. Willson, *Biotechnol. Progress* 19, 982 (**2003**).
8. Cricenti, S. Selci, A. C. Felici, R. Generosi, E. Gori, W. Djaczenko, and G. Chiarotti, *Science* 245, 1226 (**1989**).
9. V. C. Tsafack, C. A. Marquette, F. Pizzolato, and L. J. Blum, *Biosens. Bioelectron.* 15, 125 (**2000**).
10. F. Bemaudat and L. Bulow, *J. Chromatography A* 1066, 219 (**2005**).
11. H. M. Chen, W. C. Wang, and S. H. Chen, *Biotechnol. Progress* 20, 1237 (**2004**).
12. J. Maly, A. Masci, J. Masojidek, M. Sugiura, and R. Pilloton, *Anal. Lett.* 37, 1645 (**2004**).
13. E. Gizeli and J. Glad, *Anal. Chem.* 76, 3995 (**2004**).
14. J. Maly, C. Di Meo, M. De Francesco, A. Masci, J. Masojidek, M. Sugiura, A. Volpe, and R. Pilloton, *Bioelectrochemistry* 63, 271 (**2004**).
15. R. Blankespoor, B. Limoges, B. Schollhorn, J. L. Syssa-Magale, and D. Yazidi, *Langmuir* 21, 3362 (**2005**).
16. J. Maly, J. Krejci, M. Ilie, L. Jakubka, J. Masojidek, R. Pilloton, K. Sameh, P. Steffan, Z. Stryhal, and M. Sugiura, *Anal. Bioanal. Chem.* 381, 1558 (**2005**).
17. M. Nomura, T. Kobayashi, T. Kohno, K. Fujiwara, T. Tenno, M. Shirakawa, I. Ishizaki, K. Yamamoto, T. Matsuyama, M. Mishima, and C. Kojima, *FEBS Lett.* 566, 157 (**2004**).
18. D. R. Shnek, D. W. Pack, D. Y. Sasaki, and F. H. Arnold, *Langmuir* 10, 2382 (**1994**).
19. M. S. Kent, H. Yim, D. Y. Sasaki, S. Satija, J. Majewski, and T. Gog, *Langmuir* 20, 2819 (**2004**).
20. J. K. Lee, Y. G. Kim, Y. S. Chi, W. S. Yun, and I. S. Choi, *J. Phys. Chem. B* 108, 7665 (**2004**).
21. S. A. Trammel, L. Y. Wang, J. M. Zullo, R, Shashidhar, and N. Lebedev, *Biosens. Bioelectron.* 19, 1649 (**2004**).

22. K. Ng, D. W. Pack, D. Y. Sasaki, and F. H. Arnold, *Langmuir* 11, 4048 (**1995**).
23. I. T. Ahmed and A. A. A. Boraei, *Spectrosc. Lett.* 38, 47 (**2005**).
24. E. Bugella-Altamirano, J. M. Gonzalez-Perez, A. G. Sicilia-Zafra, J. Niclos-Gutierrez, and A. Castineiras-Campos, *Polyhedron* 19, 2463 (**2000**).
25. E. Bugella-Altamirano, J. M. Gonzalez-Perez, A. G. Sicilia-Zafra, J. Niclos-Gutierrez, and A. Castineiras-Campos, *Polyhedron* 18, 3333 (**1999**).
26. K. Y. Choi, H. Ryu, N. D. Sung, and M. Suh, *J. Chem. Crystal.* 33, 947 (**2003**).
27. N. C. Lim and C. Bruckner, *Chem. Commun.* 9, 1094 (**2004**).
28. M. Dakanali, E. Roussakis, A. R. Kay, and H. E. Katrinopoulos, *Tetrahedron Lett.* 46, 4193 (**2005**).
29. M. Dolaz and M. Tumer, *Transition Metal Chem.* 29, 516 (**2004**).
30. M. Shakir, S. Parveen, N. Begum, and P. Chingsubam, *Transition Metal Chem.* 29, 196 (**2004**).
31. S. Vancan, E. A. Miranda, and S. M. A. Bueno, *Process Biochem.* 37, 573 (**2002**).
32. M. Torres, J. M. Diaz-Cruz, C. Arino, B. S. Grabaric, and M. Esteban, *Electroanalysis* 11, 93 (**1999**).
33. R. L. Davidovich, I. N. Samsonova, L. V. Teplukhina, and R. N. Shchelokov, *Russian J. Coord. Chem.* 23, 327 (**1997**).
34. J. G. Kang, H. J. Kang, J. S. Jung, S. S. Yun, and C. H. Kim, *Bull. Korean Chem. Soc.* 25, 852 (**2004**).
35. W. J. Li, R. J. Wang, S. F. Si, and Y. D. Li, *J. Mol. Struct.* 694, 27 (2004).
36. D. Taratiel, J. Cabrero, C. de Graaf, and R. Caballol, *Polyhedron* 22, 2409 (**2003**).
37. H. B. Xu, L. K. Yan, Z. M. Su, S. M. Yue, H. J. Zhang, K. Z. Shao, and Y. H. Zhao, *Transition Metal Chem.* 29, 471 (**2004**).
38. B. Trzaskowski, A. Les, L. Adamowicz, P. A. Deymier, R. Guzman, and S. G. Stepanian, *J. Comput. Theor. Nanosci.*, accepted.
39. A. D. Becke, *Phys. Rev. B* 38, 3098 (**1988**).
40. C. Lee, W. Yang, and R. G. Parr, *Phys. Rev. B* 37, 785 (**1988**).
41. S. H. Vosko, L. Wilk, and M. Nusair, *Can. J. Phys.* 58, 1200 (**1980**).
42. P. C. Harihara and J. A. Pople, *Theor. Chim. Acta* 28, 213 (**1973**).
43. P. C. Harihara and J. A. Pople, *Mol. Phys.* 27, 209 (**1974**).
44. M. S. Gordon, *Chem. Phys. Lett.* 76, 163 (**1980**).
45. D. E. Woon and T. H. Dunning, *J. Chem. Phys.* 98, 1358 (**1993**).
46. R. A. Kendall, T. H. Dunning, and R. J. Harrison, *J. Chem. Phys.* 96, 6796 (**1992**).
47. T. H. Dunning, *J. Chem. Phys.* 90, 1007 (**1989**).
48. A. Schafer, H. Horn, and R. Ahlrichs, *J. Chem. Phys.* 97, 2571 (**1992**).
49. M. Dolg, U. Wedig, H. Stoll, and H. Preuss, *J. Chem. Phys.* 86, 866 (**1987**).
50. M. Dolg, H. Stoll, H. Preuss, and R. M. Pitzer, *J. Phys. Chem.* 97, 5852 (**1993**).
51. M. Cossi, N. Rega, G. Scalmani, and V. Barone, *J. Comput. Chem.* 24, 669 (**2003**).
52. M. Cossi, G. Scalmani, N. Rega, and V. Barone, *J. Chem. Phys.* 117, 43 (**2002**).
53. R. Cammi, B. Mennucci, and J. Tomasi, *J. Phys. Chem. A* 103, 9100 (**1999**).
54. B. Mennucci, E. Cances, and J. Tomasi, *J. Phys. Chem. B* 101, 10506 (**1997**).
55. S. F. Boys and F. Bernardi, *Mol. Phys.* 19, 553 (**1970**).
56. *Gaussian 03*, Revision B.05, M. J. Frisch, G. W. Trucks, H. B. Schlegel, G. E. Scuseria, M. A. Robb, J. R. Cheeseman, J. A. Montgomery, Jr., T. Vreven, K. N. Kudin, J. C. Burant, J. M. Millam, S. S. Iyengar, J. Tomasi, V. Barone, B. Mennucci, M. Cossi, G. Scalmani, N. Rega, G. A. Petersson, H. Nakatsuji, M. Hada, M. Ehara, K. Toyota, R. Fukuda, J. Hasegawa, M. Ishida, T. Nakajima, Y. Honda, O. Kitao, H. Nakai, M. Klene, X. Li, J. E. Knox, H. P. Hratchian, J. B. Cross, V. Bakken, C. Adamo, J. Jaramillo, R. Gomperts, R. E. Stratmann, O. Yazyev, A. J. Austin, R. Cammi, C. Pomelli, J. W. Ochterski, P. Y. Ayala, K. Morokuma, G. A. Voth, P. Salvador, J. J. Dannenberg, V. G. Zakrzewski, S. Dapprich, A. D. Daniels, M. C. Strain, O. Farkas, D. K. Malick, A. D. Rabuck, K. Raghavachari, J. B. Foresman, J. V. Ortiz, Q. Cui, A. G. Baboul, S. Clifford, J. Cioslowski, B. B. Stefanov, G. Liu, A. Liashenko, P. Piskorz, I. Komaromi, R. L. Martin, D. J. Fox, T. Keith, M. A. Al-Laham, C. Y. Peng, A. Nanayakkara, M. Challacombe, P. M. W. Gill, B. Johnson, W. Chen, M. W. Wong, C. Gonzalez, and J. A. Pople, Gaussian, Inc., Wallingford, CT (**2004**).

Received: 12 July 2005. Accepted: 17 July 2005.